Charge-density waves on metal surfaces

2002 J. Phys.: Condens. Matter 14 8393

(http://iopscience.iop.org/0953-8984/14/35/310)

INSTITUTE OF PHYSICS PUBLISHING JOURNAL OF PHYSICS: CONDENSED MATTER

J. Phys.: Condens. Matter **14** (2002) 8393–8414 PII: S0953-8984(02)34983-X

Charge-density waves on metal surfaces

Tetsuya Aruga

Department of Chemistry, Graduate School of Science, Kyoto University, Kyoto 606-8502, Japan

E-mail: aruga@kuchem.kyoto-u.ac.jp

Received 18 March 2002, in final form 3 May 2002
Published 22 August 2002
Online at stacks.iop.org/JPhysCM/14/8393

Abstract

Studies of the Peierls-type charge-density-wave (CDW) transitions on metal surfaces are reviewed. After the background is reviewed based on the theoretical and experimental works on such transitions in bulk quasi-low-dimensional materials, two prototypical examples are presented. One is the well known surface reconstruction transition on W(001) and Mo(001), for which there was a long-standing controversy whether the transition is due to the CDW formation or the local bonding. It is emphasized that these two pictures do not contradict each other but describe the equivocal nature of this phenomenon. The second example is the phase transition in ultrathin In films on Cu(001), which is governed by the nesting of the Fermi surface constituted by a nearly-free-electron-like sp surface resonance band, in contrast with the case of W and Mo, where much-localized d-band surface resonances play a dominant role. Finally, the origin of the long-periodicity structures widely observed in sp metals on fcc(001) systems is discussed in terms of the Fermi-surface topology expected to be common in these systems, which would be driven by strong electron–phonon coupling to lead these surfaces to the formation of the peculiar long periodicities.

1. Introduction—surface charge-density waves and nanoscience

There is now a growing interest in the surface phases which exhibit physical properties characteristic of low-dimensional systems.

Since the effects of interaction become more important in reduced dimensions, materials with highly anisotropic structures often exhibit anomalous properties such as density waves and superconductivity. At solid surfaces, the translational symmetry along one direction is broken, which implies the possibility that one may also observe properties characteristic of low-dimensional materials at solid surfaces. Such a possibility has been discussed in the past several decades for several prototypical surface systems.

Recently it has been revealed that chemically modified metal surfaces provide physical phenomena characteristic of low-dimensional materials. The In/Cu(001) [1] and Br/Pt(110) [2]

systems show structural instability due to the Fermi-surface nesting, while the substrates remain in a normal-metal state. The Fermi surfaces of these systems are constituted by two-dimensional electronic surface-resonance bands, which are not of true two-dimensional nature but are coupled, to a different extent, with three-dimensional electronic states in the bulk. The interplay of the dimensionality between three and two (or one, in the case of anisotropic surface structures) is an important feature of metal surfaces, since the dimensionality control is now well known to be a key issue in, for example, realizing high-T_c superconductors based on quasi-low-dimensional materials.

The study of such 'surface materials' is, in part, motivated by the recent technological trend toward electronic devices with nanometre-scale dimensions. As the size of the elements in devices becomes nanometre scale, quantum effects are enhanced, which would, on one hand, prevent one relying on old ideas (such as that metal is always metal, etc), but, on the other hand, lead to novel devices based on new principles. Even a nano-electronic device composed solely of 'metals', in a conventional sense, would be possible if the properties, such as the electronic states and the conductivity, of the thin films or wires of the 'metals' could be controlled by an external field.

In this review, our current knowledge about the charge-density waves (CDWs) on metal surfaces is reviewed. There had been a long-standing controversy whether the phase transitions on the (001) surfaces of W and Mo may be considered as CDW transitions or not. In particular the W(001) surface was for a long time a great touchstone for the new methodologies in surface science. Once a new technique was developed, irrespective of whether it was an experimental or theoretical one, it was applied to this surface, making the controversy look like a 'seesaw match' between two seemingly opposing pictures. We have learnt many things about the nature of CDWs, chemical bonding in extended metallic systems and so on. While some important issues are still left unsolved, the controversy seems to have been settled. The objective of this article is as follows: first, the theoretical background for the studies of CDWs is briefly summarized. Since for the bulk quasi-one-dimensional materials extensive experimental works have been performed since the early 1970s, the theoretical framework of CDWs is constructed based mainly on these results. Second, two typical surface examples are presented. One is the reconstruction of W(001) and Mo(001), which have two-dimensional Fermi surfaces of strong d character. The other is a phase transition observed in ultrathin In films on Cu(001), which have Fermi surfaces constituted by nearly-free-electron-like sp bands. A hypothesis is proposed that many long-periodicity structures observed in sp metals on the (001) surfaces of face-centred-cubic (fcc) metals are due to the electronic mechanism described essentially in terms of the concepts of CDWs in a strong-coupling regime.

2. CDW transitions in quasi-low-dimensional materials

2.1. Electron–phonon coupling

The energy-band theory has yielded remarkable success in describing the electronic structure of solids. It is, however, unlikely that the single-particle picture holds in every aspect of a solid which is comprised of a huge number of charged particles (electrons and ions). The electron–electron and electron–phonon interactions should have, to a greater or lesser extent, some effect in any real materials.

Suppose that the Hamiltonian for a conduction electron is described as $\mathcal{H} = \mathcal{H}_0 + \mathcal{H}_r$, where $\mathcal{H}_0$ describes the effective potential which gives a single-particle energy of the electron. The second term, $\mathcal{H}_r$, corresponds to the interactions (electron–electron or electron–ion) which cannot be averaged out into $\mathcal{H}_0$. There are several examples where the band theory is not a

good approximation [3]. 'Mott insulators' refers to materials which are expected to be metals within the band theory but actually are insulators due to strong electron–electron repulsion. This is a typical example of the strongly correlated systems, which are characterized by $\mathcal{H}_r$ being comparable to (or even larger than) $\mathcal{H}_0$. On the other hand, when $\mathcal{H}_r$ is so small that it can be treated as a perturbation, the effect of interaction, $\mathcal{H}_r$, is sometimes smeared out by thermal fluctuation at high temperatures. An example is superconductivity, which is realized only at low enough temperatures by a weak attractive interaction.

CDW is another example of the dramatic phenomena where the electron–phonon coupling works concertedly with the 'Fermi-surface nesting', resulting in the spatial modulation of both the conduction-electron density and the lattice of ion cores. The formation of CDWs in one-dimensional systems was first suggested by Fröhlich [4] and by Peierls [5]. Instability of a one-dimensional electron system toward a CDW state is sometimes referred to as the Peierls instability. In this and the following subsections, we give a brief account of the formation and characteristics of CDWs in solids [6, 7]. As will be shown, the CDW states in otherwise metallic materials have an origin in the instability of low-dimensional electron systems induced by the coupling of the motion of electrons with that of ion cores.

Within the band theory, the Hamiltonian $\mathcal{H}_0$ is constructed assuming that ion cores are kept still at equilibrium lattice positions, $\{R_0\}$, which is fairly well justified by the fact that the velocities of electrons are much larger than those of ions and hence the electrons experience the potential due to ions at instantaneous positions. This approximation, however, is sometimes not particularly valid and a correction is required. The effect of the thermal vibration of ions is formally treated by replacing $\{R_0\}$ with $\{R_0 + \Delta R\}$ in the formula of $\mathcal{H}_0$. Taking the lowest-order term in the expansion with respect to ΔR gives rise to $\mathcal{H}_r^{\mathrm{e-p}}$, which describes the interaction of electrons with phonons. Through this interaction, electrons are scattered by ion cores to excite phonons, and the phonons in turn exert 'external' fields on the electrons.

2.2. *Fermi-surface nesting*

Sommerfeld's electron gas model serves a very rough but clear description of metals. This is also the case for the CDW formation in metals. The point here is that the response of an electron gas to an external perturbation exhibits singularity at twice the Fermi wavevector, $2k_F$, as shown below. The discussion based on the electron-gas model suggests that the singularity is most pronounced for the particular topological structures of the Fermi surface, which would even result in the instability of the electron gas. 'Fermi-surface nesting' refers to the situation where the Fermi surface has such a topological structure.

Suppose that an electron gas is exposed to an external potential $V(r) = \int V(q) \exp(\mathrm{i}q \cdot r)\, \mathrm{d}q$. The response of the electron gas results in the rearrangement of the charge density as expressed by the induced charge density $\rho^{\mathrm{ind}}(r) = \int \rho^{\mathrm{ind}}(q) \exp(\mathrm{i}q \cdot r)\, \mathrm{d}q$. According to the Lindhard linear response theory, the response of the electron gas is described as

$$\rho^{\mathrm{ind}}(q) = \chi(q) V(q)$$

where the wavevector-dependent electron response function $\chi(q)$ is given by

$$\chi(q) = \frac{1}{V} \sum_k \frac{f(E_k) - f(E_{k+q})}{E_k - E_{k+q}} \tag{1}$$

where V denotes the volume of the system, $f(E)$ the Fermi function and E_k the electronic energy at wavevector k. At $T = 0$, $f(E_k)$ can take values of only zero or unity. The right-hand side terms of equation (1) have non-zero values only when $E_k < E_F < E_{k+q}$ or $E_{k+q} < E_F < E_k$. Hence the right-hand side of equation (1) has a large value for a pair of electrons with one just below the Fermi level and the other just above it. Figure 1 shows $\chi(q)$

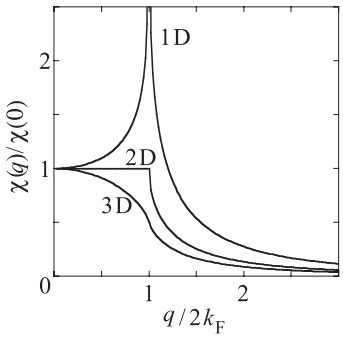

Figure 1. Response functions of one-, two- and three-dimensional free-electron gases.

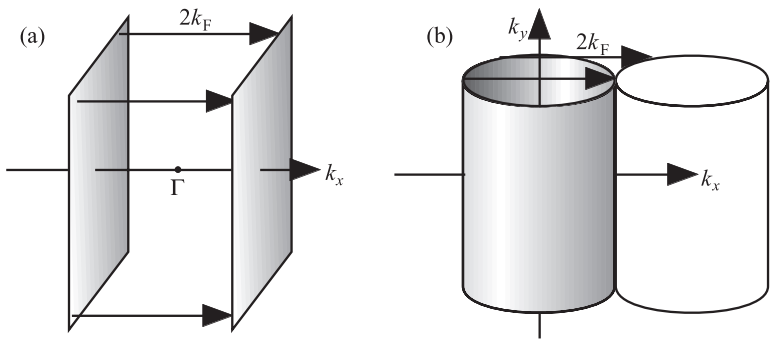

Figure 2. Fermi-surface nesting for free-electron gases in (a) one and (b) two dimensions.

at $T = 0$ as a function of q for free-electron gases of one, two and three dimensions. The singularity of $\chi(q)$ is most pronounced in one dimension, where $\chi(q)$ diverges logarithmically due to the special topology of the Fermi surface. As shown in figure 2, all the filled states at $\pm k_F$ and the empty states at $\mp k_F$ in the one-dimensional Fermi surface contribute to $\chi(q = 2k_F)$. In higher dimensions, the number of such states is much reduced.

The above scenario implies that, if there is an external perturbation with a wavevector close to $2k_F$, the electron systems with low-dimensional Fermi surfaces should undergo a divergent charge redistribution. It is the electron–phonon coupling that triggers the charge redistribution in real systems. For phonons with a wavevector $q = 2k_F$, the Hamiltonian $\mathcal{H}_r^{\mathrm{e-p}}$ surely gives such an external potential. Due to the concerted operation of the electron–phonon coupling and the Fermi-surface nesting, some low-dimensional electron–ion systems undergo periodic charge redistribution with a wavevector q, and at the same time the phonon mode at $2k_F$ is frozen in, that is, a static displacement of ion cores takes place from the equilibrium positions in the normal-metal state, which is usually referred to as periodic lattice distortion (PLD).

2.3. CDW transitions and Kohn anomaly

In order to describe the transition to the CDW state in real materials, we need both electrons and ions coupled together through the electron–phonon coupling. Theoretical modellization is sometimes performed using a nearly-free-electron-gas model coupled to the underlying chains of ions within a mean-field approximation.

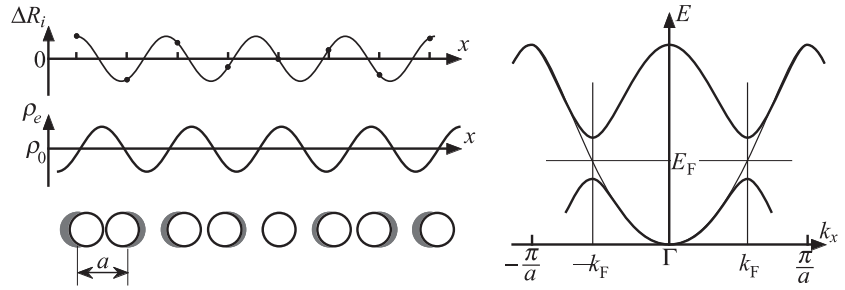

Figure 3. Lattice distortion ΔR_i, electronic charge density ρ_e, atomic structure and band structure for a one-dimensional CDW.

Figure 3 shows the mechanism of CDW formation in a one-dimensional system comprised of nearly-free electrons and a row of regularly spaced ions. In the normal-metallic state, ion cores are vibrating around the equilibrium lattice positions R_i. The thermal averages of the displacements from the equilibrium positions are zero, i.e. $\langle \Delta R_i \rangle = 0$, and the electron charge density is uniform over space, $\rho_e(x) = \rho_0$. Suppose that there is a static distortion with wavevector q. The displacement of each atom is then given by

$$\Delta R_i = R_q \cos(q R_i). \tag{2}$$

While such lattice distortion increases the strain energy of the system proportionally to $\langle \Delta R \rangle^2$, it also induces a potential for electrons, $V(q) = -g R_q$. This potential introduces a bandgap, of a size $2\Delta = 2|V(q)| = 2|g R_q|$, at $k = \pm q/2$ in the band structure. For $q = 2k_F$, the formation of a bandgap decreases the kinetic energy of the electron system. For a one-dimensional electron gas coupled with a chain of ions, the total energy change, defined by the energy cost due to the lattice distortion plus the energy gain in the electron system, has a minimum at a non-zero value of Δ, which means the realization of a CDW state. In the CDW state, both the lattice of ion cores and the electron charge density is spatially modulated with the same wavevector $q = 2k_F$. As shown in figure 3, the charge density is modulated as

$$\rho_e(x) = \rho_0 + \rho_{2k_F} \cos(2k_F x + \phi)$$

while the lattice distortion is described by equation (2) with $q = 2k_F$.

The above discussion is based on nothing but a most basic notion in band theory that an energy band has a gap at the Brillouin zone boundary. The essential point here is that the lattice distortion has a wavevector of $2k_F$, which necessarily results in energy gain in the electron system. Hence, even if the system is not of a true one-dimensional nature, the CDW transition is expected to occur in the systems with better nesting (larger overlap of the Fermi surface when shifted by $2k_F$), larger electron–phonon coupling (as measured by g) or smaller lattice strain energies (smaller phonon frequencies).

With elevating temperature, a phase transition from the CDW state to the normal-metal state should occur, since electronic as well as vibrational entropies are larger in the normal state. Within a simplified treatment based on the mean-field approximation [7], only the electronic entropy is taken into account. At elevated temperatures, the thermal excitation of electrons across the bandgap is enhanced, which degrades the energy gain due to the CDW formation and eventually drives the system into the normal state. The mean-field approximation for a weakly coupled one-dimensional electron–lattice system gives rise to the relation between the transition temperature, T_c^{MF}, and the bandgap, 2Δ, as

$$2\Delta = 3.52 k_B T_c^{MF}. \tag{3}$$

It is emphasized that this equation may be valid only for one-dimensional systems with weak electron–phonon coupling. We shall see later that real materials, bulk or surface, exhibit deviation from this equation. For two-dimensional systems, the relation between the transition temperature and Δ should also be affected by the perfection of the nesting, since the bandgap Δ cannot be uniquely defined in two dimensions but should vary in k space.

Since the transition from a high-temperature normal-metal state to a low-temperature CDW state is a second-order phase transition, a precursory phenomenon is expected to occur upon cooling down from $T > T_c^{MF}$. This is actually manifested in the softening of phonons, which is called the Kohn anomaly. The phonon frequency at a wavevector q is determined by the restoration force of the lattice against the distortion. As described above, the lattice distortion induces the potential $V(q)$ for electrons, according to which the electron charge density is temporally modulated. The charge density modulation would, in turn, weaken the restoration force of the lattice. The singularity of the susceptibility $\chi(q)$ at $q = 2k_F$ suggests that the effect is most pronounced at $q = 2k_F$. The phonon frequency, ω, of the softened mode is reduced with decreasing temperature. Within the mean-field theory, the temperature at which $\omega = 0$ is achieved corresponds to the transition temperature, T_c^{MF}. It is noted that deviation from the above simple picture is expected at temperatures near the transition temperature as discussed below.

2.4. Effects of fluctuation

Since the early 1970s, exhaustive studies have been performed on the bulk materials which undergo CDW transitions [6, 7]. Examples include a variety of quasi-one-dimensional conductors: organic charge-transfer complexes such as TTF–TCNQ (tetrathiafulvalene–tetracyanoquinodimethane), transition metal trichalcogenides such as $NbSe_3$ and TaS_3, blue bronzes such as $K_{0.3}MoO_3$ and $K_2[Pt(CN)_4X_{0.3}]nH_2O$ (X = Cl, Br). Transition metal dichalcogenides such as TaS_2 have also been a subject of recent extensive investigations of quasi-two-dimensional conductors. The transition temperatures, T_c, for most of these materials are considerably lower than expected from the mean-field equation, (3). The value of $2\Delta/k_BT_c$ is distributed in the range from 5 to 11 [7], which is rather larger than the 3.52 expected from the mean-field theory for a weakly coupled one-dimensional CDW.

It is known that no long-range order is possible in true one-dimensional systems due to the effect of fluctuation. In any *quasi*-one-dimensional materials, the CDW phases are stabilized by the interaction in higher dimensions, which is often referred to as interchain interaction. The effect of fluctuation also plays an important role in quasi-one-dimensional systems, in particular at temperatures near T_c^{MF}, which is a primary origin of the observation that the actual transition temperature is lower than T_c^{MF}. Detailed neutron and x-ray diffraction experiments for CDWs in quasi-one-dimensional materials indicated that a considerable short-range order still remains above T_c and the coherence length gradually decreases upon elevating temperature [8–10]. The revised theoretical picture suggests that, for $T_c < T < T_c^{MF}$, the free energy of the system as a function of complex order parameter Δ has a minimum at a finite $|\Delta|$ but the phase is fluctuating, and that the experimentally accessible transition temperature T_c is the temperature at which the phase eventually orders in a long range. The transition at T_c is hence considered as the result of the cooperation of lattice entropy (adiabatic term) with electronic entropy (non-adiabatic term), while the mean-field theory for weak-coupling CDWs accounts only for the latter.

It may be convenient to categorize CDWs according to the strength of the electron–phonon coupling [11,12], since the effect of fluctuation is more important in the case of strong-coupling CDWs. For the cases with weak electron–phonon coupling, which is characterized by a small

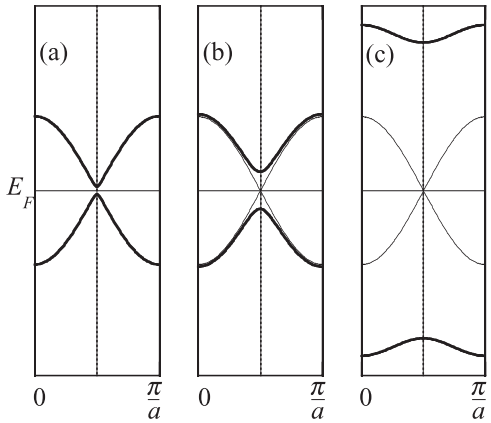

Figure 4. Schematic energy bands for (a) a weak-coupling CDW, (b) a strong-coupling CDW and (c) local bonding, for a half-filled one-dimensional metal. Thin curves show the energy band in the normal state.

value of Δ, the mean-field picture is expected to serve a good approximation of the real system. A displacive phase transition between a CDW phase and an ordered normal-metal phase should take place at a temperature close to T_c^{MF}. On the other hand, if the electron–phonon coupling is so strong that Δ is much larger than $\hbar\omega_{\mathrm{D}}$, where ω_{D} denotes the Debye frequency, a three-dimensional long-range order due to CDWs would be destroyed by lattice fluctuation at a temperature $T = T_c < T_c^{MF}$. For temperatures between T_c and T_c^{MF}, the phase and the amplitude of the PLD is fluctuating. With increasing temperature, continuous decrease of the order parameter and the coherence length should occur simultaneously, which eventually leads to the normal state above T_c^{MF}.

As suggested by McMillan [13], the CDW concept serves a natural link between the metallic bond and the ionic–covalent bond (figure 4). When the electron–phonon coupling is weak and hence the gap is small, the coherence length is quite long, corresponding to a very delocalized bond covering many metal atoms. On the other hand, when the electron–phonon coupling becomes larger, the coherence length becomes short and the bond becomes much more localized. The atomic displacement is larger and the nonlinear terms in the electron–phonon interaction tend to 'lock in' the CDWs to the lattice. At the strong-coupling limit, the metallic character disappears and the system is much more naturally described by the chemical-bond picture. Suppose that hydrogen atoms are forced to align in a one-dimensional simple lattice. When they are released from the construction, they will readily make H–H bonds to form H_2 molecules. While this process can very fairly be described as due to the Peierls instability from the viewpoint of the underlying mechanism [14], it may be appropriate to distinguish such cases from CDW transitions. A rough criterion would be the ratio of the k-space portion where the energy is gained by the CDW formation to the total volume of the first Brillouin zone. For CDWs, which are said to be stabilized by a long-range electronic effect, this ratio should be $\ll 1$. In this case, the CDW condensation energy is proportional to Δ^2. The weak-coupling CDWs are expected to be incommensurate, in general, with the parent lattice. For the cases in which the energy gap develops in most of the Brillouin zone, the phenomena would be much more naturally described by a local language, though the essential physics is the same as that for CDWs. In this case, the condensation energy is proportional to Δ and the periodicity of the ground state is determined not only by the periodicity defined by $2k_F$ but also by other factors specific to actual lattice structure and the symmetry of involved

wavefunctions etc. Hence the resulting ground state would have a strong tendency toward commensurate structures with simpler integer ratios. Actual materials lie somewhere between these two limiting cases. The strength and the q dependence of the electron–phonon coupling determines whether the CDW is commensurate or incommensurate.

3. Charge-density waves on metal surfaces

3.1. What does and does not matter on metal surfaces?

Much of our knowledge on the nature of CDWs is based on the experimental facts for the quasi-one-dimensional conductors. This class of materials have parallel one-dimensional-chain-like structures arrayed in a three-dimensional lattice. While many features are expected to be common in surface CDWs, surface systems should have their own physics because of their 'exotic' dimensionality. Let us point out several of the points peculiar to surface systems.

Coupling with bulk electronic system. Since the electronic bands of metal surfaces are, in general, in resonance with bulk electronic states, electron–phonon interaction as well as Fermi-surface nesting in the surface bands should be affected by bulk electrons. Phonon modes in surface layers should exert a potential on bulk electrons moving near the surface, leading to a situation where the stability of the surface CDW states depends on the details of the bulk band structure. The Fermi-surface nesting at a fraction of $2k_F$ observed in In/Cu(001) is closely related to this effect. For metal surfaces, excitation from bulk electronic states to the upper branch of the surface CDW bands is possible, which would reduce the CDW transition temperature from that expected for true two-dimensional systems. Another intriguing point is the penetration depth of CDW states into the bulk, which may be an important issue in the application of the metal-surface CDW to novel electronic devices.

Effect of periodic potential of substrate. In surface systems, the CDW phase may be restricted to a few atomic layers sitting on top of a crystalline substrate. The substrate potential exerts additional terms on both ions and electrons in surface layers. A most considerable effect of the substrate potential would be the strong preference toward commensurate CDWs. The periodicity determined by a Fermi wavevector is, in general, incommensurate with the substrate lattice. However, since an incommensurate surface layer is associated with a large cost in interfacial energy, a commensurate periodicity near the ideal incommensurate periodicity would be 'selected' at the expense of the energy gain due to the nesting.

Breakdown of translational symmetry along surface normal. In figure 3, a PLD is depicted as a longitudinal mode. The atomic displacement, however, is not restricted in the surface plane. It may be expected in general that transverse modes are strongly coupled with surface CDWs, because the vertical displacement of adatoms usually changes the extent of adatom–substrate charge transfer. The truncation of the three-dimensional periodicity on surfaces would also result in enhanced importance of the fluctuation effect, because the reduced bonding and symmetry at surfaces leads to softened vibrational modes.

Some of the points above may be more appropriate for metal-on-metal systems rather than for clean elemental metal surfaces, while there should be no essential difference between these two categories. Surface electronic states on modified and clean metal surfaces are, in principle, in resonance with the bulk electronic states, if not lying within the projected bulk bandgap, and hence penetrate well away from the surface into the bulk. Nevertheless, the present author

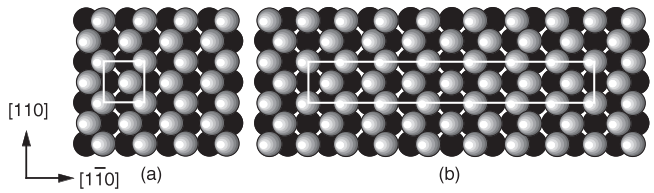

Figure 5. Structure models for (a) W(001)-($\sqrt{2} \times \sqrt{2}$)$R45^\circ$ proposed by Debe and King [22] and (b) Mo(001)-$c(7\sqrt{2} \times \sqrt{2})R45^\circ$ [33, 34].

assumes that metal-on-metal systems would exhibit a richer variety of properties characteristic of low-dimensional systems as compared with clean metal surfaces. This is because the surface resonances on metal-on-metal systems should always have a large amplitude at the surface because of its structural restriction (foreign atoms are only at the surface), while those on clean metal surfaces are often very effectively smeared out by the bulk electronic states having similar wavefunctions.

3.2. Surface reconstruction of W(001) and Mo(001)

In 1971, Yonehara and Schmidt [15] reported that the clean W(001) surface undergoes a phase transition between high-temperature (1×1) and low-temperature $c(2 \times 2)$ phases. The observation was confirmed independently by Felter *et al* [16] and Debe and King [17] in 1977. The former group also reported that the (001) surface of Mo, which is also a group-6 element like W, undergoes a similar phase transition. The low-temperature phase was reported to be incommensurate with the substrate, having a periodicity of $\sim 2.2a$ (a is the lattice constant) instead of $2a$ for W. As to the driving mechanism of the phase transition, both groups mentioned the possibility of a CDW transition. Just after these experiments, in 1978, Tosatti discussed the mechanism of the phase transitions in terms of the surface CDW [18]. He suggested in that publication that 2Δ may range from a BCS-like minimum of $3.52k_BT_c \sim 100$ meV to a maximum of perhaps one order of magnitude larger, or 1 eV, and noted that 'such a large gap is to be expected for relatively strong distorsions and short coherence lengths, a situation somewhat intermediate between conventional CDWs and the formation of ordinary chemical bond', which from the current knowledge seems to be quite appropriate.

These phase transitions have attracted a wide spread of attention and caused serious controversies in several different but related aspects of the transition, including questions of whether the transition is due to the Peierls mechanism or the local bonding, and whether the transition is displacive (order–order) or order–disorder. Early studies on these phase transitions were reviewed by King [19] and Inglesfield [20]. More recently, Jupille and King reviewed the transition on W(001) in 1994 [21], which covers most of the works performed on the W(001) phase transition to date.

3.2.1. Structure of low- and high-temperature phases. After the observation of the phase transition on W(001), Debe and King [22] further studied the LEED intensities from the low-temperature phase and deduced the space-group symmetry of $p2mg$. Based on this information, they proposed a structure model in which the top-layer W atoms are laterally displaced in the [1$\bar{1}$0] direction to form parallel zig-zag chains along the [110] direction (figure 5). This model is supported by dynamical LEED analysis [23–27], surface x-ray diffraction [28], forward-scattering photoelectron diffraction [29] and surface core-level shift [30]. It is established that the second-layer atoms are also displaced [28]. The

displacement pattern of the surface atoms can be described as zigzag chain formation or as that of the frozen-in longitudinal surface phonon mode $\bar{M}_5$ ($q = (\pi/a)(1, 1)$).

As to the low-temperature structure of Mo(001), which was first supposed to be incommensurate with the bulk periodicity, Hulpke *et al* [31] found that the surface is actually a high-order commensurate structure. The unit cell was identified as $c(7\sqrt{2} \times \sqrt{2})R45^\circ$ by LEED [32]. The structure was analysed by surface x-ray diffraction [33] and LEED [34] to yield a model in which surface Mo atoms are periodically displaced along the $[1\bar{1}0]$ direction to form a set of three zigzag chains separated by an undisplaced atomic row (figure 5). An atomistic tight-binding calculation by Roelofs and Foiles [35] also yielded a similar structure. The displacement pattern is qualitatively described as that of the longitudinal surface phonon branch the same as for W(001) but with a slightly different q vector ($q = (\pi/a)(6/7, 6/7)$ or $(\pi/a)(8/7, 8/7)$). Note that the detailed structure analyses indicated that the displacement pattern at 100 K is closer to a square wave rather than a sine wave [33] or is temperature dependent [34].

The (001) surfaces of both W and Mo undergo phase transitions to (1×1) at $\sim$220 K for W [36] and $\sim$150 K for Mo [37]. While there was a controversy as to whether the transition is order–order (displacive) or order–disorder, it now seems to be well established that, at temperatures around 300 K, the surface atoms on the W(001) surface are not on the (1×1) lattice positions but are laterally displaced to nearly the same extent as in the low-temperature phase. The phase transition at $\sim$220 K is hence of order–disorder nature as indicated by He atom diffraction [38], LEED [25], surface core-level shift [30], high-energy ion scattering [39], surface x-ray diffraction [36, 40] and forward-scattering photoelectron diffraction [29]. This is also the case for Mo(001) [41, 42].

Terakura *et al* [43, 44] calculated the energy changes caused by the reconstruction using a tight-binding model with a recursion method for very large cluster models mimicking W(001) and Mo(001). Their result indicated that the surface is unstable toward the longitudinal distortion mode corresponding to the Debe–King model. The calculated surface density of states showed a considerable splitting of a d-band peak, which is observed at E_F for the ideal (1×1) structure, to two components above and below E_F. They further calculated [45] the surface response function with and without electron–phonon matrix elements. The result indicated the importance of the electron–phonon coupling in this reconstruction. The stability of the Debe–King model has been supported by many other calculations. The total energy of the $c(2 \times 2)$ surface is calculated to be stabilized by 60 [46] to 100–110 meV [47, 48] per surface atom as compared with the (1×1) structure, which suggests that the transition temperature of 220 K is too low to be accounted for by a simple displacive, order–order transition, and that the surface just above T_c must have a disordered character [47, 49, 50].

While the disorder nature of the surface around room temperature was sometimes invoked as contradicting with the CDW concept, this may be based on too narrow a definition of CDWs. As briefly described in section 2.4, the breakdown only of the long-range order at a temperature lower than T_c^{MF} can be well described within the CDW concept, assuming that the coherence length is short (due to the Peierls gap in an extended portion in k space induced by strong electron–phonon coupling) and that the dominant entropy is the lattice entropy, as originally suggested for CDWs in 2H–$TaSe_2$ [13]. Hence, in order to give a quantitative account of the mechanism of this transition from the structural viewpoint, one has to study the temperature dependence of the degree of disorder up to much higher temperatures. However, the experimental structural analyses of this surface to date are limited to 300–450 K in most works. While the high-energy ion scattering data up to 600 K were suggested to support the 'disordered' character of the surface even at 600 K [39], it was claimed that the data are also consistent with the ordered (1×1) structure [51]. Many works have been performed

by simulation methods using effective interatomic potential models [52–58]. Roelofs and Wendelken [53] discussed the Debye–Waller behaviour of LEED intensity.

An unsolved discrepancy lies between the results of He atom diffraction and those of other diffraction experiments. The He atom diffraction results show the existence of an intermediate phase, with degraded long-range order and an incommensurate periodicity, between the low-temperature c (2×2) and high-temperature (1×1) phases [38, 51, 59–61]. This intermediate phase, however, was not observed by Ne atom diffraction [60], surface x-ray diffraction [36, 40] or LEED [62, 63]. The origin of the discrepancy has been discussed by several authors [12, 38, 51, 60, 64–66]. In particular, Ernst *et al* [51] suggested that an incommensurate CDW phase is actually realized in the intermediate temperature range while at the same time the amplitude of the associated PLD is smaller than the detection limit of the x-ray diffraction (∼0.05 Å) [36]. A two-stage CDW transition with an intermediate incommensurate phase is known to take place, for example, in $K_{0.3}MoO_3$ [7, 10], in which case, however, PLD in the intermediate phase was clearly observed by x-ray diffraction.

3.2.2. Dynamical behaviour of the phase transition. Inelastic He atom scattering has provided information on the phonon softening and the dynamical critical behaviour of W(001) [51,59,65] and Mo(001) [65, 67, 68]. The dispersion of the longitudinal surface phonon on W(001) and Mo(001) was measured for wide ranges of surface temperature above T_c. The considerable softening of the longitudinal phonon was observed at $\sim 0.8\bar{\mathrm{M}}$, beyond which no significant inelastic structure was observed. Ernst *et al* [51] gave an extensive discussion on the dynamics of the transition on W(001) and suggested that above ∼450 K the surface is essentially (1×1), as evidenced by the well defined longitudinal surface phonon. They also suggested that the broadening of the phonon peak below 450 K is indicative that the surface atoms are displaced from (1×1) positions and are dynamically disordered. Their view on the transition qualitatively agrees with that suggested by Roelofs *et al* [52], who, using the Migdal renormalization-group method and a Monte Carlo coarse-graining calculation, suggested the crossover between order and disorder behaviour and the non-displacive character of surface atoms at higher temperatures.

Fasolino and Tosatti [69] and Wang *et al* [70, 71] studied the vibrational properties of W(001) by a molecular dynamics method. It was shown that the longitudinal and shear horizontal modes, which are related to the reconstruction, show critical broadening and softening upon approaching the transition temperature [71]. The temperature dependences of the phonon energies were in good agreement with that observed by He atom scattering [51]. The shear horizontal mode, which determines the phase of the $c(2 \times 2)$ order, was shown to be responsible for the phase fluctuations near the transition temperature.

Han *et al* [72,73] studied theoretically the critical dynamics of the W(001) phase transition by using a combination of analytical and Monte Carlo simulation methods. A remarkable agreement with the experiment [51] was obtained for the dispersion of the longitudinal surface phonon on W(001). The experimentally observed softening behaviour was reproduced. The phonon energy approaching zero at $\sim 0.8\bar{\mathrm{M}}$ and the disappearance beyond this wavevector above T_c was ascribed to the overdamping due to the critical fluctuation induced by the strong anharmonic effect near the transition temperature. Their simulation also showed a 'central peak' [74–78] due to the diffusive motion of ordered domains, which however was not evident in the He scattering spectra [51]. As to the structure of the surface at higher temperatures, Han *et al* [72] showed that the probability distribution of the mean-square displacement on each site exhibits a peak at a non-zero displacement even at $T = 5T_c$, while the peak approaches zero with increasing temperature. This indicates that the surface may have a considerable 'disordered' character even at $T \sim 1000$ K as opposed to the undisplaced (1×1) structure invoked based on the observation of well defined phonon peaks.

3.2.3. Electronic structure and mechanism of the phase transition. Wang and Weber [79] and Wang *et al* [80] studied the reconstruction mechanism of W(001) and Mo(001), respectively, by using a non-orthogonal tight-binding (NTB) scheme for the electronic structure and electron–phonon matrix elements [81, 82]. They analysed the phonon dispersion, which showed a softening at $\bar{\mathrm{M}}$ for W(001) and a maximum instability at $0.83\bar{\mathrm{M}}$ for Mo(001), in good agreement with the low-temperature periodicities observed on these surfaces. They further calculated the 'bare' electronic susceptibility $\chi_0(q)$ and that modulated with the electron–phonon matrix elements. The origin of the phonon instabilities was addressed to the coupling with the $\bar{\Sigma}_2$ surface electronic band. While $\chi_0(q)$ shows its maximum close to $q = 2k_F$, the q dependence of the electron–phonon matrix elements controls the actual q value at which the phonon instability occurs. The low-temperature reconstruction of W(001) and Mo(001) is thus understood as realized by the competition between the $2k_F$ effect, represented by $\chi_0(q)$, and the electron–phonon matrix elements, which reflect the real-space features of the atomic arrangement and wavefunction symmetry and are strongly q dependent, in particular for d bands, and favour higher-order commensurability.

Note that the above picture does not necessarily contradict the local-bonding picture. It is the strength of the electron–phonon coupling that locates the system somewhere between the weak-coupling CDW as hypothesized in the mean-field theory and the purely local chemical bonding.

As to the dispersion of the $\bar{\Sigma}_2$ surface state, a good overall agreement among theoretical calculations is established for W(001)-(1 × 1): the surface-state band is located at 0.5–0.8 eV below E_F at $\bar{\Gamma}$, shows flat but slightly upward dispersion along $\bar{\Sigma}$, crosses the Fermi level at $\sim 0.6\bar{\mathrm{M}}$ and disperses up to 2–2.5 eV above E_F at $\bar{\mathrm{M}}$ [48,83–89]. The calculations for Mo(001) also show similar results [89,90]. According to the NTB calculation by Wang and Weber [79], a bandgap of ∼0.3 eV is generated at $\bar{\mathrm{M}}$ in the low-temperature $c(2 \times 2)$ structure of W(001), indicating that the CDW in this system may be classified into the strong-coupling regime. On the other hand, their calculation shows that the gapping extends to ∼40% of the $\bar{\Sigma}$ axis, indicating a very short coherent length, ∼10 Å, which suggests that the local bonding picture is also appropriate. Note that the self-consistent calculations by Bullet and Stephenson [85], Drube *et al* [91] and Yu *et al* [48] show larger bandgaps of 1.1–1.7 eV, while the k-space portions affected by the transition are similar to that calculated by Wang and Weber.

The experimental verification of the electronic structure would serve as critical information on the mechanism of the phase transitions. Results of angle-resolved photoemission (ARPES) have been reported for W(001) [92–94] and Mo(001) [95–98]. Angle-resolved inverse photoemission (ARIPES) experiments have also been carried out [91,99,100]. The determined dispersion relations for the surface state (resonance) near the Fermi level are in gross agreement with the calculated ones. However, because of the finite energy resolution of the experiments (100–150 meV in ARPES and 300–600 meV in ARIPES), the behaviour of the surface band close to the Fermi level is not well resolved, which prevents the critical assessment of the validity of the theoretical results. Besides, since the measurements for the high-temperature phase were made at 300–320 K, at which temperature the surface is disordered and may contain many small domains of the $c(2 \times 2)$ structure, the observed dispersion may not directly be ascribed to the non-displaced (1 × 1) structure. The calculation of the density of states for a one-dimensional system with fluctuation taken into account [101] showed a pseudogap at $T < T_c^{MF}$, which might suggest that the band structure measured at 300 K for W(001) and Mo(001) is affected by the fluctuation and has characteristic features similar to those of the low-temperature phase. While the band structure and the Fermi surface below T_c were also measured and extensively discussed for Mo(001) [97, 98] and W(001) [94], the comparison with the theoretical calculations for the transition mechanism is not very convincing.

As a final remark, the reconstruction transitions on W(001) and Mo(001) are well described within the framework of the d-electron chemical bonding between adjacent surface atoms and at the same time these are also properly described by the language of CDW with strong electron–phonon coupling. In view of the opinion that the CDW argument is more appropriate for the systems with coherent length much longer than the normal-state lattice constant, one may chose the chemical bonding concept to describe these systems. On the other hand, in order to understand the correlation among the low-temperature structure, the phonon dynamics and the surface electronic structure in a straightforward way, it is convenient to discuss these in terms of the CDW concept.

3.3. Monolayers of sp-block metallic elements on Cu(001)

The reconstruction on W(001) and Mo(001) is due to the d-band effect, local or non-local in nature. The d band is characterized by gradual dispersion and the tendency toward localized behaviour. An example with a totally opposite character was recently presented: the surface CDW due to the Fermi-surface nesting of a nearly-free-electron-like sp surface resonance band.

3.3.1. In on Cu(001): brief introduction. Many 4p and 5p post-transition metals have structures which can be described as distorted from high-symmetry structures such as fcc and bcc. One of Peierls' original motivations to propose the concept of the Peierls instability was to explain some such distorted structures [5]. These elements are close to the boundary between metals and non-metals, which would imply strong electron–phonon coupling. Indium is a metallic element in such a category and has a $[Kr]4d^{10}5s^24p^1$ electron configuration and a distorted fcc (formally described as body-centred tetragonal) structure. On the other hand, copper has a $[Ar]3d^{10}4s^1$ electron configuration. The d-band maximum is located $\sim$2 eV below E_F and hence only sparse sp bands exist around E_F. On the (001) surface of Cu, there is a large projected bandgap around $\bar{M}$. These features of Cu(001) would imply that the interaction of Cu(001) with metallic overlayers is more weakly corrugated than that in the case of early transition metal surfaces. The large size mismatch between Cu and In is another factor of this system. The metallic diameter of In, 3.25 Å, is $\sim$30% larger than that of Cu, 2.56 Å, which would smear out the corrugation effect of the substrate potential and elicit a faint electronic effect as structural transformation of the overlayers.

Figure 6 shows the phase diagram of In/Cu(001) [102]. The system gives rise to seven long-range-ordered phases in the coverage range $\theta_{In} < 1.0$ (the coverage is defined so that $\theta_{In} = 1.0$ corresponds to the atomic density of Cu(001)). The low-temperature phases, $c(3\sqrt{2}\times\sqrt{2})R45^\circ$ and $(5\sqrt{2}\times 5\sqrt{2})R45^\circ$, are metastable and transform irreversibly to room-temperature phases upon annealing.

At room temperature, initial In deposition leads to the incorporation of In atoms into the topmost layer. Upon further In deposition, the dealloying transition occurs at around $\theta_{In} = 0.3$, which leads to an In overlayer on top of the Cu surface. The $(9\sqrt{2} \times 2\sqrt{2})R45^\circ$ structure is completed at $\theta_{In} = 0.5$, which, upon heating, transforms reversibly to $c(2 \times 2)$ $((\sqrt{2} \times \sqrt{2})R45^\circ)$ at $T = 350$ K. Further increase of In coverage at 300 K leads to successive formation of two ordered phases, $c(4 \times 4)$ $((2\sqrt{2} \times 2\sqrt{2})R45^\circ)$ at $\theta_{In} = 0.63$ and $(\sqrt{20} \times \sqrt{20})R63.4^\circ + p(2 \times 2)$ at $\theta_{In} = 1.0$. Upon heating, both phases transform reversibly at around $T = 450$ K to $p(2 \times 2)$. The high-resolution STM images for some of these ordered phases are shown in figure 7 [102].

3.3.2. Valence electronic structure of In/Cu(001). The ARPES spectra measured with He I radiation at an emission angle corresponding to the $\bar{X}$ point are shown in figure 8 [103], in

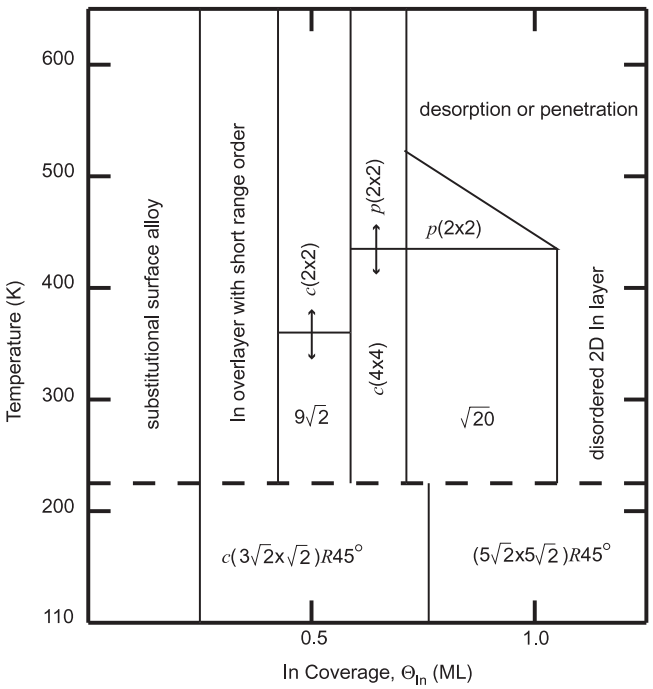

Figure 6. Phase diagram for In/Cu(001) [102]. '$9\sqrt{2}$' and '$\sqrt{20}$' denote the $(9\sqrt{2}\times 2\sqrt{2})R45^\circ$ and $(\sqrt{20}\times\sqrt{20})R63.4^\circ + p(2\times 2)$ phases, respectively. The $c(3\sqrt{2}\times\sqrt{2})R30^\circ$ and $(5\sqrt{2}\times 5\sqrt{2})R45^\circ$ phases are metastable and can be achieved only by deposition below 200 K. The broken line indicates irreversible phase transitions, while the solid lines with arrows at both ends indicate reversible transitions.

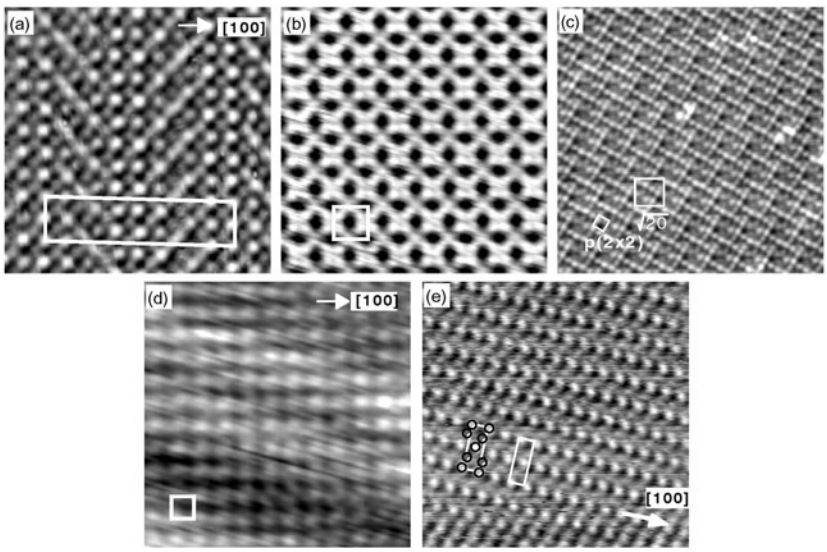

Figure 7. Atomically resolved STM images of In/Cu(001) for (a) $(9\sqrt{2}\times 2\sqrt{2})R45^\circ$ (40×40 Å^2), (b) $c(4\times 4)$ (58×58 Å^2), (c) $(\sqrt{20}\times\sqrt{20})R63.4^\circ + p(2\times 2)$ (105×105 Å^2), (d) $c(2\times 2)$ (40×40 Å^2) and (e) $c(3\sqrt{2}\times\sqrt{2})R45^\circ$ (58×58 Å^2) [102].

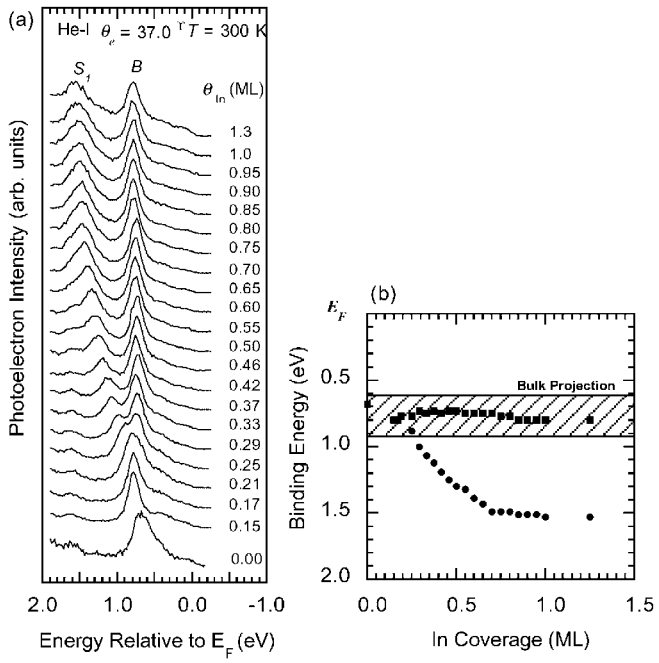

Figure 8. (a) ARPES spectra at $\bar{X}$ as a function of In coverage at 300 K. S_1 denotes the In-induced surface resonance and B the bulk Cu 4sp band [103]. (b) Binding energy for the S_1 (circles) and Cu 4sp (squares) bands at $\bar{X}$ as a function of In coverage. The hatched area indicates the projected bulk Cu 4sp band at $\bar{X}$.

which the peak due to the bulk sp band of Cu is designated as B. Upon In deposition at 300 K, a new peak, designated as S_1, appears at around $\theta_{In} = 0.25$, shifts downward in energy with increasing θ_{In} and asymptotically approaches the saturation value of ∼1.5 eV. An important point is the variation of the intensity, which increases at the initial stage, reaches a maximum at $\theta_{In} \sim 0.65$ and then decreases significantly above $\theta_{In} \sim 1$, suggesting that the state is highly localized at the Cu–In interface. (The weak feature around 1.6 eV is due to the excitation of the Cu 3d band by He I_β.)

The ARPES measurement was made to trace the S_1 peak throughout the surface Brillouin zone [1, 103]. The S_1 peak runs mostly parallel with the edge of the projected bulk 4sp band of Cu and was ascribed to the formation of an interfacial state between Cu 4sp and In 5sp states. Figure 9 shows schematically the two-dimensional dispersion of the S_1 band for the $c(2 \times 2)$ phase, the high-temperature phase at $\theta_{In} = 0.5$. The S_1 band can be approximated by a two-dimensional nearly-free-electron band and gives rise to a squarelike Fermi surface around $\bar{M}$. Roughly speaking, the whole energy band is shifted to higher binding energies with increasing coverage, resulting in the shrinking of the Fermi surface around $\bar{M}$. It is to be noted that the saddle-point structure at $\bar{X}$ is due to the hybridization gap. The upper branch constitutes another Fermi surface (electron pocket) around $\bar{X}$, which was not clearly observed with He I [103] but was studied thoroughly with synchrotron radiation at $h\nu = 80$ eV [104].

3.3.3. Fermi-surface nesting and structural transitions in In/Cu(001). The mechanism of the reversible transitions, those between $(9\sqrt{2} \times 2\sqrt{2})R45^\circ$ and $c(2 \times 2)$ [1] and between $c(4 \times 4)$ and $p(2 \times 2)$ [104], have been studied by ARPES. Figure 10 shows the Fermi surface

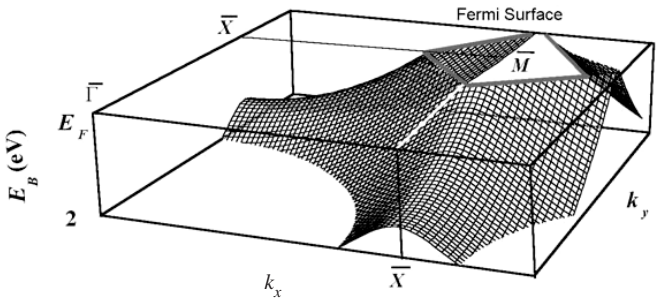

Figure 9. Schematic representation of the two-dimensional dispersion of the surface resonance band, S_1, for Cu(001)–$c(2 \times 2)$-In.

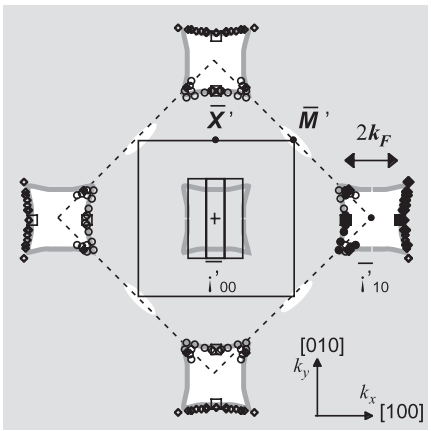

Figure 10. Fermi surface of the $c(2 \times 2)$ phase [1]. Solid symbols denote data taken under different conditions. Open symbols are generated by mirror operation. The grey lines enclosing the $\bar{\Gamma}'$ points show Fermi surfaces generated according to the $c(2 \times 2)$ translational symmetry in the extended zone scheme. The solid lines represent the SBZ of $c(2 \times 2)$ (large square) and $(9\sqrt{2} \times 2\sqrt{2})R45^\circ$ (small rectangles). Also shown is the surface Brillouin zone of Cu(001)-(1×1) with the dashed lines. The shaded region shows the Cu bulk Fermi surface projected onto Cu(001)-(1×1). $\bar{\Gamma}'_{00}$–$\bar{\Gamma}'_{10} = 1.74$ Å^{-1}.

determined by ARPES for the $c(2 \times 2)$ phase [1]. The shaded area shows the Cu bulk Fermi surface projected onto the (001)-(1×1) plane. The surface Fermi surface runs very close to the edge of the projected bulk Fermi surface. Note that the projected bandgaps around $\bar{M}$ do not actually exist on the $c(2 \times 2)$ surface. Also shown is the surface Brillouin zone of the low-temperature $(9\sqrt{2} \times 2\sqrt{2})R45^\circ$ phase. While the sides of the first Brillouin zone do not coincide with the Fermi surface, the boundaries of the next zone do. This indicates that a fractional nesting condition, $Q = 2k_F/3$, is fulfilled.

Whether or not the surface resonance band is really nested in the low-temperature phase was examined by directly comparing the band dispersion for the surfaces above and below the transition temperature. Figure 11(b) shows the ARPES spectra for the high-temperature $c(2 \times 2)$ and the low-temperature $(9\sqrt{2} \times 2\sqrt{2})R45^\circ$ phases along the $\bar{M}'$–$\bar{\Gamma}'_{10}$ ($\bar{X}$–$\bar{M}$) axis. The k_x value marked for each curve, in the unit of Å^{-1}, indicates the momentum component parallel to $\bar{\Gamma}'_{00}$–$\bar{\Gamma}'_{10}$ ($\bar{\Gamma}$–$\bar{M}$). While the S_1 band crosses E_F in the high-temperature phase, for the LT phase the S_1 band does not cross E_F but turns back down to higher binding energies.

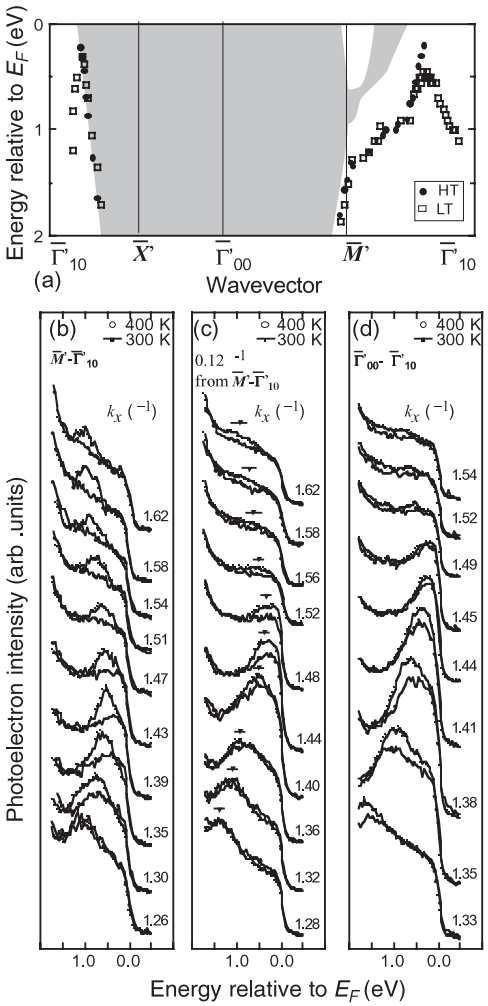

Figure 11. (a) Valence band structure of In/Cu(001) at $\theta_{\text{In}} = 0.5$ [1]. The data obtained with $h\nu = 22.78$ eV are shown. Filled circles are for the high-temperature $c(2 \times 2)$ phase and open squares for the low-temperature $(9\sqrt{2} \times 2\sqrt{2})R45^\circ$ phase. Angle-resolved photoelectron spectra for $c(2\times2)$ ($T = 400$ K) and $(9\sqrt{2}\times2\sqrt{2})R45^\circ$ ($T = 300$ K) phases: (b) along $\bar{\text{M}}'$–$\bar{\Gamma}'_{10}$; (c) along the line parallel to $\bar{\text{M}}'$–$\bar{\Gamma}'_{10}$ and shifted off by 0.12 Å^{-1}; (d) along $\bar{\Gamma}'_{00}$–$\bar{\Gamma}'_{10}$. The momentum components along the [100] direction, k_x, are indicated.

As far as the present author is aware, this is the sole observation to date of the band back-folding due to the Fermi-surface nesting. The binding energy at the turning-back point is ∼400 meV, which suggests that quite a large bandgap opens in the low-temperature phase.

The magnitude of the bandgap depends on the position in reciprocal space as found in the spectra taken along the line parallel to $\bar{M}'$–$\bar{\Gamma}'_{10}$ but shifted off by 0.12 Å^{-1} (figure 11(c)) and along $\bar{\Gamma}'_{00}$–$\bar{\Gamma}'_{10}$ (figure 11(d)). The bandgap is most significant at the corners of the Fermi surface and is very small (or not formed) at the centre of the sides. It may appear that the folded-back component of the S_1 band is observed, though the intensity is very weak, even in the high-temperature phase. It might be probable that the short-range order due to the CDW is remanent at 400 K due to the fluctuation effect.

A question may arise why the symmetry breaking was observed not at $2k_F$ but at a fraction of $2k_F$. It is to be emphasized that the $2k_F$ mode, among infinite numbers of possible $2k_F/N$ modes, does not necessarily give the ground state in real systems. While in 1987 Kennedy and Lieb [105] proved rigorously that the $2k_F$ mode is exact for a special one-dimensional model, there is no strict rule for the general cases of the Peierls-type instability, in particular for non-one-dimensional systems, as to which of the $2k_F/N$ modes gives the ground state. In the present case, it is possible to assume that the energy cost in the Cu bands, in the near-surface region, is high for a PLD corresponding to $2k_F$, since the Cu bands should also experience the new periodicity and contribute to the total energy change.

The band dispersions of the S_1 band for high- and low-temperature phases are shown in figure 11(a). It is emphasized that the dispersion curves mostly coincide with each other except for the small k-space portion near the Fermi surface, which is in a strong contrast with the cases of W(001), for which the calculated band for the low-temperature phase is strongly affected over ∼50% of the surface Brillouin zone. This difference may be forwarded to the sp character of the In/Cu Fermi surface as opposed to the d character in the case of W and Mo.

The band structure suggests a rather long coherence length in the In/Cu(001) system, as opposed to the short value, ∼10 Å, in the reconstructed structure of W(001). The $(9\sqrt{2} \times 2\sqrt{2})R45^\circ$ periodicity in the In/Cu(001) system is considered as due to the Peierls-type CDW transition induced by the cooperation of the nesting of the sp-character Fermi surface and the electron–phonon coupling. While the relatively large maximum bandgap, $\Delta_{max} \sim 400$ meV, may suggest that this CDW be categorized into the strong-coupling ones, quantitative theoretical investigations are desirable for the two-dimensional systems with a varying bandgap. The dynamical structure of the high-temperature phase is also intriguing. While the STM image taken at 400 K (figure 7) shows a well ordered $c(2 \times 2)$ structure, this might be due to the time averaging of a dynamically fluctuating surface. On the other hand, the ARPES result implies that the fluctuation effect is small. Quantitative investigation of the dynamical behaviour would reveal the role of fluctuation in this system.

The study of the $c(4 \times 4)$–$p(2 \times 2)$ transition shows that the shrunk Fermi surface around $\bar{\mathrm{M}}$ results in the different commensurate periodicity and that the partial-nesting feature is more enhanced in this case [104].

3.3.4. Relevance to the other sp-metal-on-Cu(001) systems. An interesting speculation is that the band structures of other sp-metal/Cu(001) systems should resemble that of In/Cu(001) as shown in figure 9 and hence give rise to Fermi surfaces similar to that shown in figure 10. If so, Fermi-surface nesting in the $\bar{\Gamma}$–$\bar{\mathrm{M}}$ direction is also expected for many systems, while the periodicity may vary according to the length of the spanning vector. Thus, the structures with general formulae of $c(n\sqrt{2} \times \sqrt{2})R45^\circ$ or $(n\sqrt{2} \times 2\sqrt{2})R45^\circ$, n an odd integer, for one-dimensional nesting and $p(n\sqrt{2} \times n\sqrt{2})R45^\circ$, $n = 2$ or an odd integer, for two-dimensional nesting are expected. In the literature, such structures are found not only in several sp-metal/Cu(001) systems but also on the (001) surfaces of Ag, Au and Ni as listed in table 1. Models for some of the structures are consistent with the picture that the $c(2 \times 2)$ (or $p(2 \times 2)$) structures are modulated in the [100] direction, while the 'modulation' here includes the slight periodic displacement of the atom positions as well as the periodic insertion of dislocations, the latter being understood as due to real-space effects as for the discommensurations in incommensurate structures [126]. It is quite possible that these large-unit-cell structures are stabilized by the Fermi-surface nesting with strong electron–phonon coupling, as is the case for $(9\sqrt{2} \times 2\sqrt{2})R45^\circ$ and $(2\sqrt{2} \times 2\sqrt{2})R45^\circ$ in In/Cu(001). It is also noted that structures with different formulae, such as Cu(001)–(10×10)-Bi [120], may also be understood by the Fermi-surface-induced long-range periodic modulation along the [100] and [010] directions of the

Table 1. Structures possibly explained by strongly coupled CDW.

Substrate	Adsorbate	Structure	References
Cu(001)	Li	$c(5\sqrt{2}\times\sqrt{2})R45^\circ$	[106]
		$c(7\sqrt{2}\times\sqrt{2})R45^\circ$	[106]
	In	$(2\sqrt{2}\times 2\sqrt{2})R45^\circ$	[1, 102]
		$(5\sqrt{2}\times 5\sqrt{2})R45^\circ$	[102]
		$c(3\sqrt{2}\times\sqrt{2})R45^\circ$	[102]
		$(9\sqrt{2}\times 2\sqrt{2})R45^\circ$	[1, 102]
	Tl	$(2\sqrt{2}\times 2\sqrt{2})R45^\circ$	[107, 108]
		$(6\sqrt{2}\times 2\sqrt{2})R45^\circ$	[109, 110]
	Pb	$(2\sqrt{2}\times 2\sqrt{2})R45^\circ$	[111–114]
		$c(5\sqrt{2}\times\sqrt{2})R45^\circ$	[111–118]
	Bi	$(2\sqrt{2}\times 2\sqrt{2})R45^\circ$	[119]
		$c(9\sqrt{2}\times\sqrt{2})R45^\circ$	[119, 120]
Ag(001)	Na	$c(5\sqrt{2}\times\sqrt{2})R45^\circ$	[106]
		$c(7\sqrt{2}\times\sqrt{2})R45^\circ$	[106]
		$c(9\sqrt{2}\times\sqrt{2})R45^\circ$	[106]
	Bi	$(2\sqrt{2}\times 2\sqrt{2})R45^\circ$	[121]
		$c(3\sqrt{2}\times\sqrt{2})R45^\circ$	[121]
Au(001)	Pb	$c(3\sqrt{2}\times\sqrt{2})R45^\circ$	[122, 123]
		$c(7\sqrt{2}\times\sqrt{2})R45^\circ$	[122, 123]
Ni(001)	Li	$c(5\sqrt{2}\times\sqrt{2})R45^\circ$	[124]
		$c(9\sqrt{2}\times\sqrt{2})R45^\circ$	[106]
	Pb	$c(5\sqrt{2}\times\sqrt{2})R45^\circ$	[125]

$c(2\times 2)$ (or $p(2\times 2)$) structures. The present author believes that temperature-dependent experiments, which have scarcely been performed for these systems even by LEED, are desirable for the systematic understanding of the origin of these structures.

Among these structures, some structures observed in the Tl/Cu(001) system, including $(6\sqrt{2}\times 2\sqrt{2})R45^\circ$, have already been claimed to be due to the Peierls instability [108–110]. It was assumed that Tl atoms are arrayed to form one-dimensional chains along the [110] direction [107, 127, 128]. The ARPES spectra taken along the assumed chain direction ($\bar{\Gamma}$–$\bar{\mathrm{X}}$) were interpreted to be consistent with the bandgap formation at E_F in the low-temperature phase [109]. Since Tl and In are in the same group in the periodic table, let us briefly comment on the results for Tl/Cu(001). The Tl-induced surface resonance, which was observed at a photon energy of $h\nu = 7.87$ eV to cross the Fermi level at $\sim 0.5\bar{\mathrm{X}}$ [109], seems to correspond in the case of In/Cu(001) to the upper branch above the hybridization gap around $\bar{\mathrm{X}}$, which is not shown in figure 9. This branch was very weak and diffuse when photons with $h\nu \sim 20$ eV were used [1, 103], but was clearly observed at 80 eV photon energy to run parallel with that observed in Tl/Cu(001) [104]. In the case of In/Cu(001), the Fermi surface constituted by this band (an electron pocket around $\bar{\mathrm{X}}$) was not affected by the phase transition. It was the hole pocket around $\bar{\mathrm{M}}$ that exhibited considerable Fermi-surface nesting upon transition. At the moment we do not have any ARPES data for the hole pocket around $\bar{\mathrm{M}}$ in the case of Tl/Cu(001). It is not even proven whether such a hole pocket really exists in Tl/Cu(001). However, the similarity of Tl and In in electronic structure and chemical nature would imply that the phase transition in Tl/Cu(001) is also related to the Fermi surface around $\bar{\mathrm{M}}$. Clearly, this problem should be addressed in a future work.

4. Concluding remark

In this paper, we have concentrated on the studies of two prototypical metal surfaces. There are, however, several recent topics closely related to the matter dealt with in this paper. The Br/Pt(110) system [2] has presented another example of the metal-surface CDW. On semiconductors, several surfaces have been proposed to undergo surface CDW transitions. The origin of the phase transitions observed in Pb(Sb)/Ge(111) was suggested to be surface CDWs [129, 130], which has been one of the hottest topic in surface science in the past several years. More recently, metallic linear chains of In on Si(111) were shown to undergo a CDW transition [131], where the nesting of the quasi-one-dimensional Fermi surface, formed within the projected bulk bandgap, was shown to drive the transition.

The situation is rather surprising, since such phenomena have been eagerly sought for more than 30 years in the field of surface science, which yielded only very limited success until recently. It may be the developments in the methodology for the characterization of electronic properties, atomic as well as mesoscopic structure of surfaces that have enabled these new discoveries, which, obviously, are now opening a new important field of 'surface materials science'. The present author believes that a further pursuit of novel surface systems with intriguing properties and the measurements of macroscopic properties such as the conductivity of these materials will cultivate the field as a fruitful ground for nanomaterials science.

References

[1] Nakagawa T, Boishin G I, Fujioka H, Yeom H W, Matsuda I, Takagi N, Nishijima M and Aruga T 2001 *Phys. Rev. Lett.* **86** 854
[2] Swamy K, Menzel A, Beer R and Bertel E 2001 *Phys. Rev. Lett.* **86** 1299
[3] Ashcroft N W and Mermin N D 1976 *Solid State Physics* (Fort Worth: Harcourt Brace)
[4] Fröhlich H 1954 *Proc. R. Soc.* A **223** 296
[5] Peierls R E 1955 *Quantum Theory of Solids* (Oxford: Clarendon) p 108
[6] Kagoshima S, Nagasawa H and Sanbongi T 1988 *One-Dimensional Conductors* (Berlin: Springer)
Kagoshima S, Sanbongi T, Nagasawa H and Takahashi T 2000 *Teijigen-Doutai* [*Low-Dimensional Conductors*] (Tokyo: Shokabo)
[7] Grünner G 1994 *Density Waves in Solids* (Reading, MA: Addison-Wesley)
[8] Pouget J P, Kagoshima S, Schlenker C and Marcus J 1983 *J. Physique* **44** L113
[9] Pouget J P, Noguera C, Moudden A H and Moret R 1985 *J. Physique* **46** 1731
Pouget J P, Noguera C, Moudden A H and Moret R 1986 *J. Physique* **47** 147 (erratum)
[10] Pouget J P and Comes R 1989 *Charge Density Waves in Solids* ed L P Gor'kov and G Grüner (Amsterdam: North-Holland) p 85
[11] Tosatti E 1980 *Modern Trends in the Theory of Condensed Matter (Lecture Notes in Physics 115)* ed A Pekalski and J Przystawa (Berlin: Springer) p 501
[12] Tosatti E 1995 *Electronic Surface States and Interface States on Metallic Systems* ed E Bertel and M Donath (Singapore: World Scientific) p 67
[13] McMillan W L 1977 *Phys. Rev.* B **16** 643
[14] Hoffmann R 1988 *Solids and Surfaces: a Chemist's View of Bonding in Extended Structures* (New York: Wiley) p 4
[15] Yonehara K and Schmidt L D 1971 *Surf. Sci.* **25** 238
[16] Felter T E, Barker R A and Estrup P J 1977 *Phys. Rev. Lett.* **38** 1138
[17] Debe M K and King D A 1977 *J. Phys. C: Solid State Phys.* **10** L303
[18] Tosatti E 1978 *Solid State Commun.* **25** 637
[19] King D A 1983 *Phys. Scr.* T **4** 34
[20] Inglesfield J E 1985 *Prog. Surf. Sci.* **20** 105
[21] Jupille J and King D A 1994 *The Chemical Physics of Solid Surfaces* vol 7, ed D A King and D P Woodruff (Amsterdam: Springer) p 35
[22] Debe M K and King D A 1977 *Phys. Rev. Lett.* **39** 708
[23] Debe M K and King D A 1979 *Surf. Sci.* **81** 193

[24] Walker J A, Debe M K and King D A 1981 *Surf. Sci.* **104** 405
[25] Pendry J B, Heinz K, Oed W, Landskron H, Müller K and Schmidtlein G 1988 *Surf. Sci.* **193** L1
[26] Landskron H, Bickel N, Heinz K, Schmidtlein G and Müller K 1989 *J. Phys.: Condens. Matter* **1** 1
[27] Schmidt G, Zagel H, Landskron H, Heinz K, Müller K and Pendry J B 1992 *Surf. Sci.* **271** 416
[28] Altman M S, Estrup P J and Robinson I K 1988 *Phys. Rev.* B **38** 5211
[29] Lee J, Huang D-J and Erskine J L 1995 *Phys. Rev.* B **51** 13 824
[30] Jupille J, Purcell K G and King D A 1989 *Phys. Rev.* B **39** 6871
[31] Hulpke E and Smilgies D-M 1991 *Phys. Rev.* B **43** 1260
[32] Hildner M L, Daley R S, Felter T E and Estrup P J 1991 *J. Vac. Sci. Technol.* A **9** 1604
[33] Smilgies D-M, Eng P J and Robinson I K 1993 *Phys. Rev. Lett.* **70** 1291
[34] Daley R S, Felter T E, Hildner M L and Estrup P J 1993 *Phys. Rev. Lett.* **70** 1295
[35] Roelofs L D and Foiles S M 1993 *Phys. Rev.* B **48** 11 287
[36] Robinson I K, MacDowell A A, Altman M S, Estrup P J, Evans-Lutterrodt K, Brock J D and Birgeneau R J 1989 *Phys. Rev. Lett.* **62** 1294
[37] Felter T E 1984 *J. Vac. Sci. Technol.* A **2** 1008
[38] Salanon B and Lapujoulade 1986 *Surf. Sci.* **173** L613
[39] Stensgaard I, Purcell K G and King D A 1989 *Phys. Rev.* B **39** 897
[40] Evans-Lutterrodt K, Birgeneau R J, Specht E D, Chung J W, Brock J D, Altman M S, Estrup P J, Robinson I K and MacDowell 1989 *J. Vac. Sci. Technol.* A **7** 2209
[41] Kelly D G, Lin R F, Van Hove M A and Somorjai G A 1989 *Surf. Sci.* **224** 97
[42] Hildner M L, Daley R S, Felter T E and Estrup P J 1995 *Phys. Rev.* B **52** 9050
[43] Terakura K, Terakura I and Teraoka Y 1979 *Surf. Sci.* **86** 535
[44] Terakura I, Terakura K and Hamada N 1981 *Surf. Sci.* **111** 479
[45] Terakura I, Terakura K and Hamada N 1981 *Surf. Sci.* **103** 103
[46] Fu C L and Freeman A J 1988 *Phys. Rev.* B **37** 2685
[47] Singh D, Wei S-H and Krakauer H 1986 *Phys. Rev. Lett.* **57** 3292
[48] Yu R, Krakauer H and Singh D 1992 *Phys. Rev.* B **45** 8671
[49] Roelofs L D 1986 *Phys. Rev.* B **34** 3337
[50] Singh D and Krakauer H 1988 *Phys. Rev.* B **37** 3999
[51] Ernst H-J, Hulpke E and Toennies J P 1992 *Phys. Rev.* B **46** 16 081
[52] Roelofs L D, Hu G Y and Ying S C 1983 *Phys. Rev.* B **28** 6369
[53] Roelofs L D and Wendelken J F 1986 *Phys. Rev.* B **34** 3319
[54] Wang C Z, Parrinello M, Tosatti E and Fasolino A 1988 *Europhys. Lett.* **6** 43
[55] Wang C Z, Tosatti E and Fasolino A 1988 *Phys. Rev. Lett.* **60** 2661
[56] Roelofs L D, Ramseyer T, Taylor L L, Singh D and Krakauer H 1989 *Phys. Rev.* B **40** 9147
[57] Han W K and Ying S C 1990 *Phys. Rev.* B **41** 9163
[58] Yoshimori A 1991 *Prog. Theor. Phys.* **106** 433
[59] Ernst H-J, Hulpke E and Toennies J P 1987 *Phys. Rev. Lett.* **58** 1941
[60] Schweizer E K and Rettner C T 1989 *Surf. Sci.* **208** L29
[61] Ernst H-J, Hulpke E and Toennies J P 1989 *Europhys. Lett.* **10** 747
[62] Wendelken J F and Wang G-C 1985 *Phys. Rev.* B **32** 7542
[63] Bauer E, unpublished (cited in [51])
[64] Estrup P J, Robinson I K and Tully J C 1989 *Surf. Sci.* **215** L297
[65] Hulpke E 1990 *J. Electron Spectrosc. Relat. Phenom.* **54/55** 299
[66] Man'kovsky S V and Cherepin V T 1996 *Surf. Sci.* **352–354** 711
[67] Hulpke E and Smilgies D-M 1989 *Phys. Rev.* B **40** 1338
[68] Hulpke E and Smilgies D-M 1990 *Phys. Rev.* B **42** 9203
[69] Fasolino A and Tosatti E 1987 *Phys. Rev.* B **35** 4264
[70] Wang C Z, Fasolino A and Tosatti E 1987 *Phys. Rev. Lett.* **59** 1845
[71] Wang C Z, Fasolino A and Tosatti E 1988 *Phys. Rev.* B **37** 2116
[72] Han W K, Ying S C and Sahu D 1990 *Phys. Rev.* B **41** 4403
[73] Han W K and Ying S-C 1992 *Phys. Rev.* B **46** 1849
[74] Riste T, Samuelson E J, Otnes K and Feder J 1971 *Solid State Commun.* **9** 1455
[75] Feder J 1971 *Solid State Commun.* **9** 2021
[76] Shirane G and Axe J D 1971 *Phys. Rev. Lett.* **27** 1803
[77] Shapiro S M, Axe J D, Shirane G and Riste T 1972 *Phys. Rev.* B **6** 4332
[78] Krumhansl A and Schriefer J R 1975 *Phys. Rev.* B **11** 3535
[79] Wang X W and Weber W 1987 *Phys. Rev. Lett.* **58** 1452

[80] Wang X W, Chan C T, Ho K M and Weber W 1988 *Phys. Rev. Lett.* **60** 2066
[81] Varma C M, Blount E I, Vashishta P and Weber W 1979 *Phys. Rev.* B **19** 6130
[82] Varma C M and Weber W 1979 *Phys. Rev.* B **19** 6142
[83] Krakauer H, Posternak M and Freeman A J 1979 *Phys. Rev. Lett.* **43** 1885
[84] Posternak M, Krakauer H, Freeman A J and Koelling D D 1980 *Phys. Rev.* B **21** 5601
Posternak M, Krakauer H, Freeman A J and Koelling D D 1984 *Phys. Rev.* B **30** 4828(E)
[85] Bullet D W and Stephenson P C 1983 *Solid State Commun.* **45** 47
[86] Ohnishi S, Freeman A J and Wimmer E 1984 *Phys. Rev.* B **29** 5267
[87] Mattheiss L F and Hamann D R 1984 *Phys. Rev.* B **29** 5372
[88] Cherepin V T, Floka V M, Man'kovsky S V, Ostroukhov A A and Tomilenko V N 1994 *J. Electron Spectrosc. Relat. Phenom.* **68** 105
[89] Legoas S B, Araujo A A, Laks B, Klautau A B and Frota-Pessôa 2000 *Phys. Rev.* B **61** 10 417
[90] Hong S C and Chung J W 1993 *Phys. Rev.* B **48** 4755
[91] Drube W, Straub D, Himpsel F J, Soukiassian P, Fu C L and Freeman A J 1986 *Phys. Rev.* B **34** 8989
[92] Smith K E, Elliot G S and Kevan S D 1990 *Phys. Rev.* B **42** 5385
[93] Elliott G S, Smith K E and Kevan S D 1991 *Phys. Rev.* B **44** 10 826
[94] Shin K S, Kim H W and Chung J W 1997 *Surf. Sci.* **385** L978
[95] Smith K E and Kevan S D 1991 *Phys. Rev.* B **43** 3986
[96] Smith K E and Kevan S D 1992 *Phys. Rev.* B **45** 13 642
[97] Chung J W *et al* 1992 *Phys. Rev. Lett.* **69** 2228
[98] Shin K S, Kim C Y, Chung J W, Hong S C, Lee S K, Park C Y, Kinoshita T, Watanabe M, Kakizaki A and Ishii T 1993 *Phys. Rev.* B **47** 13 594
[99] Collins I R, Laine A D and Andrews P T 1992 *J. Phys.: Condens. Matter* **4** 2891
[100] Lamouri A and Krainsky I L 1994 *Surf. Sci.* **303** 341
[101] Lee P A, Rice T M and Anderson P W 1973 *Phys. Rev. Lett.* **31** 462
[102] Nakagawa T, Mitsushima S, Okuyama H, Nishijima M and Aruga T 2002 *Phys. Rev.* B at press
[103] Nakagawa T, Okuyama H, Nishijima M and Aruga T, submitted
[104] Nakagawa T *et al*, submitted
[105] Kennedy T and Lieb E H 1987 *Phys. Rev. Lett.* **59** 1309
[106] Tochihara H and Mizuno S 1998 *Prog. Surf. Sci.* **58** 1
[107] Binns C and Norris C 1982 *Surf. Sci.* **115** 395
[108] Binns C, Barthés-Labrousse M G and Norris C 1984 *J. Phys. C: Solid State Phys.* **17** 1465
[109] Binns C and Norris C 1991 *J. Phys.: Condens. Matter* **3** 5425
[110] Binns C, Norris C and Barthes-Labrousse M-G 1992 *Phys. Scr.* T **45** 283
[111] Henrion J and Rhead G E 1972 *Surf. Sci.* **29** 20
[112] Sepulveda A and Rhead G E 1977 *Surf. Sci.* **66** 436
[113] Nagl C, Platzgummer E, Haller O, Schmidt M and Varga P 1995 *Surf. Sci.* **331–333** 831
[114] Robert S, Cohen C, L'Hoir A, Moulin J, Schmaus D and Barthes-Labrousse M G 1996 *Surf. Sci.* **365** 285
[115] Bibérian J P and Huber M 1976 *Surf. Sci.* **55** 259
[116] Hösler W and Moritz W 1986 *Surf. Sci.* **175** 63
[117] Sánchez A and Ferrer S 1989 *Phys. Rev.* B **39** 5778
[118] Li W, Lin J-S, Karimi M and Vidali G 1991 *J. Vac. Sci. Technol.* A **9** 1707
[119] Delamare F and Rhead G E 1972 *Surf. Sci.* **35** 172
[120] Meyerheim H L, De Santis M, Moritz W and Robinson I K 1998 *Surf. Sci.* **418** 295
[121] Saito Y, Nakagawa T, Ogami O, Okuyama H, Nishijima M and Aruga T, at press
[122] Biberian J P and Rhead G E 1973 *J. Phys. F: Met. Phys.* **3** 675
[123] Biberian J-P 1978 *Surf. Sci.* **74** 437
[124] Jiang H, Mizuno S and Tochihara H 1997 *Surf. Sci.* **385** L930
[125] Perdereau J and Szymerska I 1972 *Surf. Sci.* **32** 247
[126] McMillan W L 1976 *Phys. Rev.* B **14** 1496
[127] Binns C, Newstead D A, Norris C, Barthes-Labrousse M G and Stephenson P C 1986 *J. Phys. C: Solid State Phys.* **19** 829
[128] Binns C, Nicklin C L, Barthes-Labrousse M-G and Norris C 1991 *J. Phys.: Condens. Matter* **3** 3041
[129] Carpinelli J M, Weitering H H, Plummer E W and Stumpf R 1996 *Nature* **381** 398
[130] Carpinelli J M, Weitering H H, Bartkowiak M, Stumpf R and Plummer E W 1997 *Phys. Rev. Lett.* **79** 2859
[131] Yeom H W *et al* 1999 *Phys. Rev. Lett.* **82** 4898